LTD-18
PA 218-235

Simplified patterning of Mo/Cu transition edge sensors

D. McCammon, F. T. Jaeckel, K. Nelms, C.V. Ambarish, A. Roy

University of Wisconsin Madison, 1150 University Avenue, Madison 53706 USA

Abstract

Superconducting/normal metal layer bilayers with tunable T_c are widely used as transition edge sensors in high-resolution microcalorimeters. When these layers are patterned, channels with enhanced T_c (compared to the bilayer) form along the edges of the device where the superconductor is only partially covered by normal metal. Superconductivity near the edges can be suppressed by deposition of additional normal metal to cover the exposed superconducting edges. Alternatively, the same effect can be obtained by producing an overhang in the normal metal of the bilayer by using an isotropic etch to undercut the superconductor. For Mo/Cu bilayers, however, producing a reliable undercut with a wet etch proved difficult due to electrochemical corrosion of copper in the presence of molybdenum. We are trying out an all-dry etch process to achieve the desired geometry. This achieves the desired results, but we are still working on complete characterization of the etch. This is also part of an effort to reduce longitudinal proximity and weak link effects by minimizing the amount of material with much higher or lower T_c in contact with the bilayer, which should simplify the transition behavior and improve reproducibility. We are experimenting with devices that have no normal metal zebra stripes and use a minimum volume of molybdenum (T_c = ~1 K) rather than niobium (T_c = ~9 K) for the contacts.

1. Introduction

- A careful comparison of the metals produced by stars and supernovae 2 billion years after the big-bang and current observations shows us that we see only 20% of the total metals produced. (the **missing metals** problem).
- Majority of these are thought to reside in the Circum-galactic medium (CGM) and the Warm-Hot Interstellar Medium (WHIM). Their high metallicity environments make X-ray observations one of the best ways to study them.
- Astrophysical plasmas at temperatures close to $1x10^6$ K are ubiquitous. Substantial parts of the Galactic halo and disk appear to be at this temperature, including most of the volume within 100 pc of the Sun (The Local Hot Bubble).
- Bulk of the emission from these plasmas are at 600 eV or lower. To better understand the physics of the ISM, we need to be able to resolve the individual lines from such a plasma (and there are a lot of them).

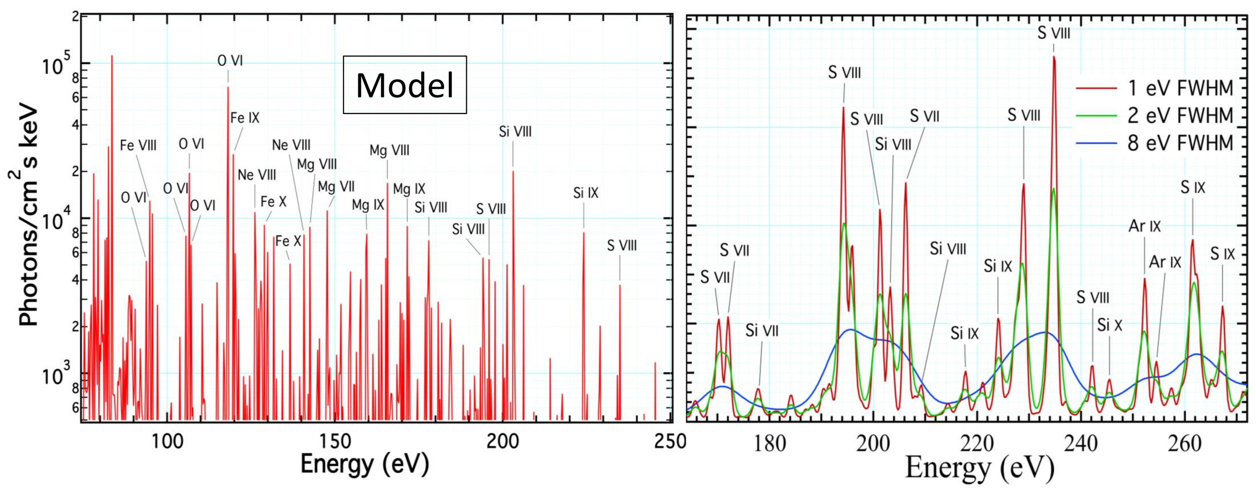

The above figure shows a simulation of a model spectra with 1, 2 and 8 eV FWHM detectors. 1 eV detectors are essential to be able to clearly resolve the individual lines at lower energy. That is our goal.

2. Design Specifications

The energy resolution of a microcalorimeter is proportional to $(T^2C\sqrt{k}/\alpha)^{1/2}$, where k is the modification to the Johnson noise term defined as $k \equiv (1+2\beta_I)(1+M^2)$, M being an "excess" noise term of unknown origin, determined empirically. Here, $\alpha \equiv \partial lnR/\partial lnT$ and $\beta_I \equiv \partial lnR/\partial lnI$ are the usual definitions of logarithmic current and temperature dependence of TES resistance respectively. This implies we should minimize the total heat capacity C and operating temperature T and maximize thermometer sensitivity.

Getting a small heat capacity will be limited by the large X-ray absorber required. To achieve a total effective area of > 2 cm² with 256 pixels, we need X-ray absorbers of about 1 mm² size with good stopping efficiency over our primary energy range.

A 500 eV X-ray will raise the temperature of our 1 pJ/K detector by 80 μK. Assuming α = 400 at 10% R_n, the transition has a width of 1800 μK, and the excursion is <4% of the transition. *(Always linear!)*

- $I_{c,0}$ scales with the effective device width with a slope ~0.25 mA/μm (**Morgan 2017**)
- Using two-fluid model of TESs, and for device effective width of 135 μm, scaling $I_{c,0}$ to 32 mA we expect $\alpha \sim 470, \beta \sim 2$

Green line in plot indicates where TES devices made with this fabrication process land on the contour.

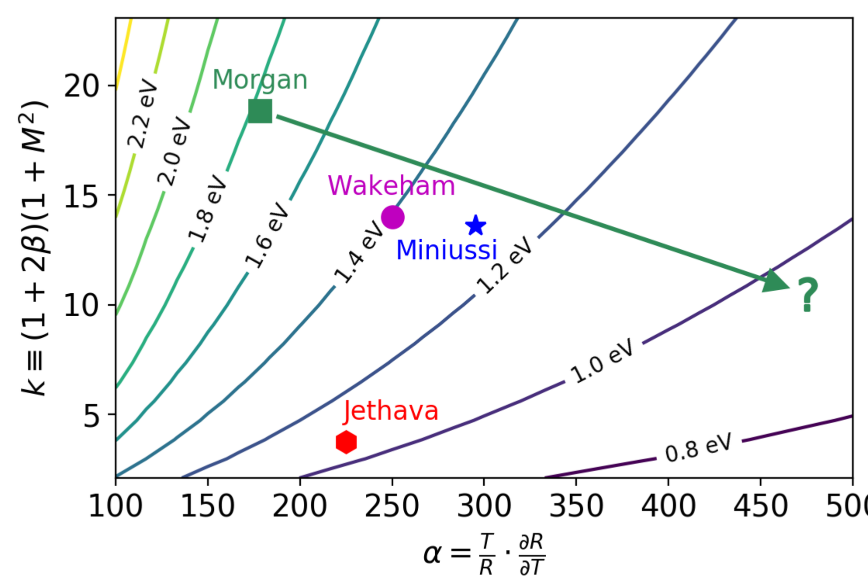

The FWHM energy resolution contours are generated with T_{BASE} = 50 mK, T_{BIAS} = 70 mK, $C_{(TBIAS)}$ (absorber) = 1.0 pJ/K, C_{TES} = 0.21 pJ/K, $G_{TES\text{-}BATH}$ = 35 pW/K, $G_{ABS\text{-}TES}$ = 1 μW/K, and $G_{electron\text{-}phonon}$ (within the TES) = 10 nW/K.

3. TES Fabrication

Bilayer Fabrication

- We have developed an alternative deposition approach using low energy ion beam assisted deposition (IAD) that does not require heating of the substrate and results in controllable stress as well as a clean superconductor/normal metal interface (**Morgan et al. 2015, Jaeckel et al. 2016**).
- Ion beam energy and flux give us additional *knobs* to tweak and good control over film density and stress.

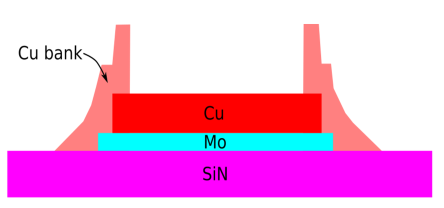

- Commonly encountered challenges in the fabrication of arrays include variations in T_c and other details of the transition surface from run-to-run and between neighboring devices.
- Evidence suggests that to some extent these result from process variation, e.g. misalignment between different lithography steps of TES fabrication (**Wakeham et al. 2018B**).
- The usual process requires at least two lithography steps to pattern the bilayer, and a third to produce the banks to keep the device from shorting out along the edges. A final device is illustrated on the left

- We propose to further develop an alternative "self-aligned" process that defines the all-important lateral boundaries of the TES from a single mask. The process in illustrated on the schematic on the right.
  1. An argon ion-mill step first produces trenches through the Cu along the sides of TES.
  2. It is followed by a pulsed XeF_2 gas phase etch that only etches the Mo and produces a controllable undercut of the Mo so that edges remain fully proximitized and do not short out the device.
  3. Subsequent wet etch steps remove the bulk of the unwanted Mo and Cu material between the devices, but do not come into contact with the critical sidewalls of the TES. This avoids any electro-galvanic corrosion issues which we encountered with wet-etching of Mo (**Nelms et al. 2003**).
- We expect much improved repeatability as a result.

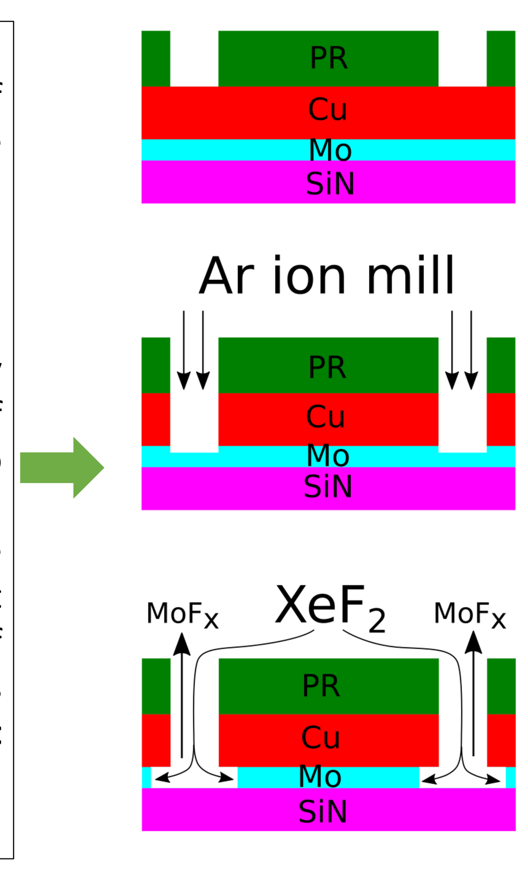

4. Absorber Fabrication

Gold, and why?

Gold has excellent thermalization properties for rapidly turning the X-ray photon energy to heat, a very high thermal diffusivity which will be important for the large absorbers. The Goddard group has a well-developed process for making gold-based "mushroom" absorbers. So despite its high specific heat, our baseline design calls for an all-gold absorber.

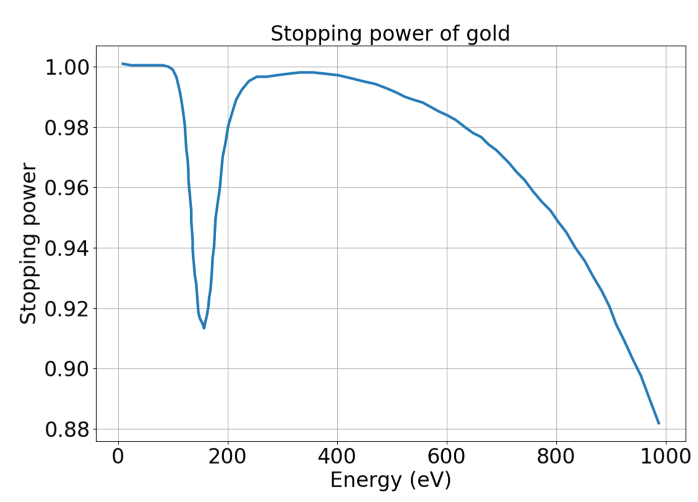

Figure above shows that a 200 nm layer of gold is still 99% efficient at stopping X-rays upto 500 eV (**Hencke, 1993**)

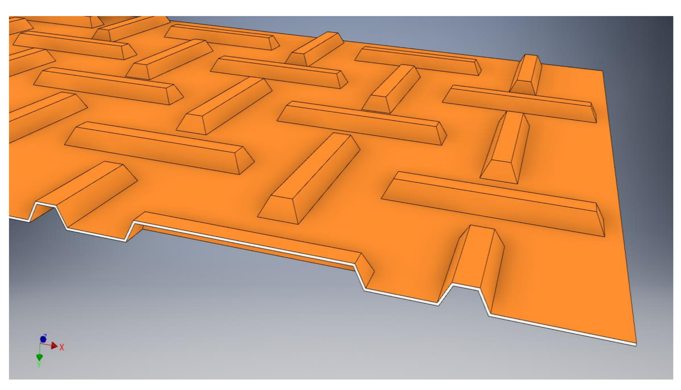

Cut-away view of the proposed gold absorber structure (not to scale). Corrugations provide bi-directional stiffening.

a)

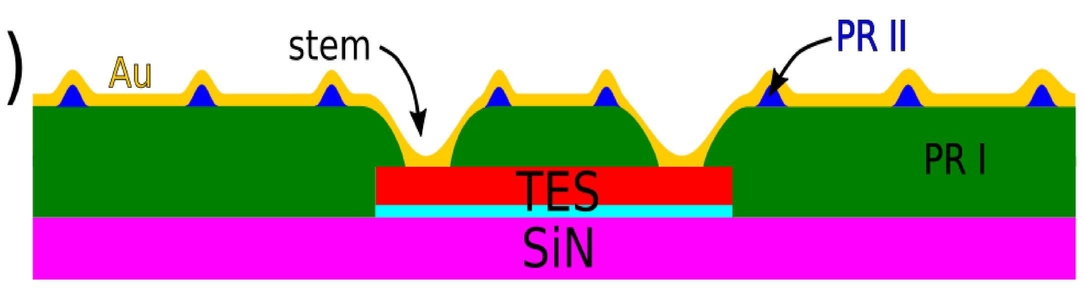

Openings are patterned in a first photoresist layer (PR I) for the absorber stems. This first layer is then hard-baked to produce rounded sidewalls and render it stable against further exposure. PR layer II is then spun and patterned with the intended corrugation pattern (with the stem area once again opened to the TES). Another heat treatment reflows the photoresist to have the desired angled sidewalls. Gold is evaporated onto this "mold". To obtain good sidewall coverage, the substrate can be held at an angle on a rotating platform

b)

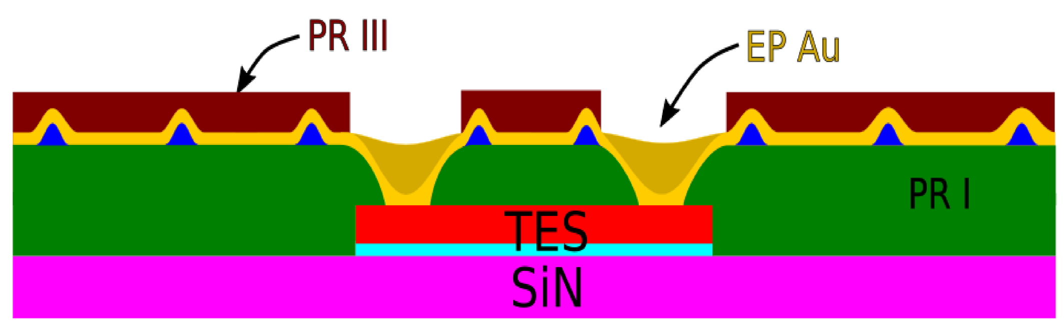

Next, a third layer of photoresist (PR III) is coated on the Au and patterned to again expose the stem area. Gold electroplating fills and strengthens the stems.

c)

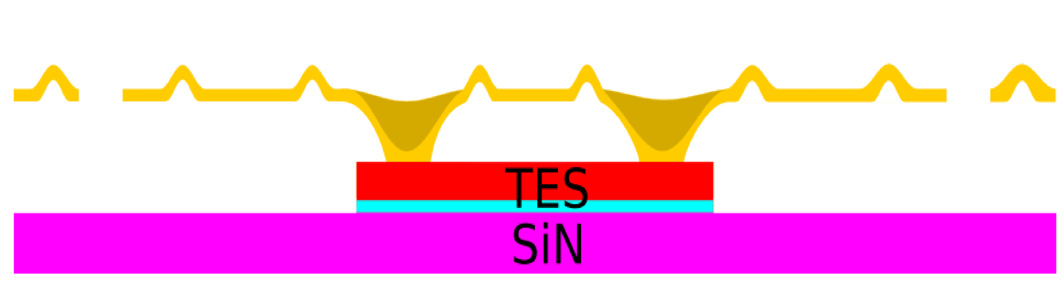

In the final step, the photoresists are dissolved away and we are left with free-standing orthogonally corrugated gold absorbers attached to the TESs via stems.

Acknowledgements

This work was supported in part by NASA grant NNX13AH21G. The authors would like to thank the Nanoscale Fabrication Center (NFC), and Nanoscale Imaging and Analysis Center (NIAC) at University of Wisconsin-Madison for use of their facilities.

References

1. Morgan, K. M *et al.* (2017) "*Dependence of transition width on current and critical current in transition-edge sensors*," Appl Phys Letters 110, 212602.
2. Morgan, K. M., Jaeckel, F. T., Kripps, K. L., McCammon, D. 2015a, "*Ion-Beam-Assisted Deposition of Mo Thin Films for TES Applications*," IEEE Trans. Appl. Supercond. 25, 2101505
3. Wakeham, N *et al.* (2018b), "*The Impact of Transition Edge Sensor Design on Achievable Performance Uniformity of Kilo-Pixel Arrays*", Applied Superconductivity Conference 2018, NASA NTRS GSFC-E-DAATN62871
4. Nelms, K. L., Ali, S., Dosaj, A., Liu, D., McCammon, D., Rocks, L. E., Sanders, W. T., Timbie, P., and Vaillancourt,J.E. (2003), "*Microelectronic Fabrication of Transition Edge Sensors*," Microscopy and Microanalysis, 9(S02), 122- 123,